KLOE Memo 344

June 2008

Updates on the measurement of the $e^+e^- \to \omega\pi^0 \to \pi^0\pi^0\gamma$ cross section using 2001-2006 data

A. De Santis[a], S. Giovannella[b], S. Miscetti[b]

[a] *Università "La Sapienza" and Sezione INFN, Roma, Italy*

[b] *Laboratori Nazionali di Frascati dell'INFN, Frascati, Italy*

Abstract

In this note, we report the measurement of the visible cross section for $e^+e^- \to \omega\pi^0 \to \pi^0\pi^0\gamma$ events performed using 450 pb^{-1} of e^+e^- collisions collected in the 2001−2002 data taking period, together with the 2005 scan data (four energy points of $\sim$ 10 pb^{-1} each) and $\sim$ 106 pb^{-1} of the 2006 off-peak data. We study the dependence of the cross sections on the center of mass energy in the range 1000−1030 MeV and fit it to extract the relevant parameters of the process.

1 Introduction

In the analysis of the $e^+e^- \to \pi^0\pi^0\gamma$ process with 2001/2002 data [1] it was shown that two contributions dominates: the resonant $\phi \to S\gamma$ decay ($S\gamma$), where S is a light scalar meson, and the non-resonant reaction $e^+e^- \to \omega\pi^0$ ($\omega\pi$). The fit to the $\pi^0\pi^0\gamma$ Dalitz plot indicated than the contribution of the interference between these two terms is practically negligible, so that it is possible to separate $S\gamma$ and $\omega\pi$ events. This was already done using 2001/2002 data in [2], where the visible cross section of the two processes was studied as a function of the center of mass energy ($\sqrt{s}$). We have now added to our old data set the four points of the 2005 scan data, about 10 pb^{-1} each and a fraction ($\sim$ 106 pb^{-1}) of the 2006 off-peak data. The larger spanning of $\sqrt{s}$ obtained including 2005/2006 data allows the determination of all the parameters describing the non-resonant process, while in the past only the behaviour around M_ϕ was reliably extracted.

This study, together with the analogous work on $e^+e^- \to \omega\pi^0 \to \pi^+\pi^-\pi^0\pi^0$, provides the most precise measurements of the $\Gamma(\omega \to \pi^0\gamma)/\Gamma(\omega \to \pi^+\pi^-\pi^0)$ ratio and of the main ω branching fractions [3].

2 Analysis summary for 2001/2002 data

The analysis performed on 2001/2002 data is extensively described in [2]. Here we just recall the most important points. Data were mainly collected at $\sqrt{s} \sim M_\phi$, with center of mass energies having a spread of about 2 MeV, and with two additional off-peak data sets (1017 and 1022 MeV). All data are grouped in $\sqrt{s}$ bins of 100 keV. The analysis is then performed for bins with an integrated luminosity of at least 1 pb^{-1}.

The two processes that contributes to the $\pi^0\pi^0\gamma$ final state at $\sqrt{s} \sim M_\phi$ are the non-resonant $e^+e^- \to \omega\pi^0$ and the ϕ radiative decays $\phi \to S\gamma$, where S is both $f_0(980)$ and $\sigma(600)$. The ratio of the visible cross sections is $\sigma(\omega\pi)/\sigma(S\gamma) \approx 2$. The main background channels are:

1. $\eta\pi\gamma$: $\phi \to a_0(980)\gamma \to \eta\pi^0\gamma$ with $\eta \to \gamma\gamma$;
2. $\eta\gamma_7$: $\phi \to \eta\gamma$ with $\eta \to \pi^0\pi^0\pi^0$ that mimics the signal because of lost or merged photons;
3. $\eta\gamma_3$: $\phi \to \eta\gamma$ with $\eta \to \gamma\gamma$ that mimics the signal because of cluster splitting or accidental coincidence of machine background events.

The first step of the analysis is the sample selection, requiring events with five neutral clusters in the expected time window (TW), defined as $|T_\gamma - R_\gamma/c| < \mathrm{MIN}(5\,\sigma_T, 2\text{ ns})$. T_γ and R_γ are the reconstructed time and position of the cluster, while σ_T is the time resolution. The cutoff at 2 ns reduces the contribution of accidental coincidence with low energy background clusters. In the photon counting, energy and angular acceptance cuts are applied. Only clusters with $E_\gamma > 7$ MeV and $|\cos\theta_\gamma| < 0.92$ are considered. $e^+e^- \to \gamma\gamma(\gamma)$ events are then removed by requiring $E_1 + E_2 < 900$ MeV, where $E_{1,2}$ are the energies of the two most energetic clusters.

For events surviving the sample selection, a three steps procedure for pairing photons into π^0's has been developed:

Background	$\mathrm{S/B_{nocuts}}$	$\mathrm{S/B_{sele}}$	$\mathrm{S/B_{final}}$
$\phi \to \eta\pi^0\gamma \to \gamma\gamma\pi^0\gamma$	8.5	8.8	18.9
$\phi \to \eta\gamma \to \pi^0\pi^0\pi^0\gamma$	0.1	0.5	3.9
$\phi \to \eta\gamma \to \gamma\gamma\gamma$	0.1	18.8	32.3

Table 1: Signal over background ratio for events with $\sqrt{s} \sim M_\phi$, evaluated at different steps of the analysis: before any requirements (nocuts), after sample selection (sele) and after background rejection (final).

1. kinematic fit applied to the five photon sample, requiring energy-momentum conservation and time of flight for each photon;
2. parametrization of the photon energy resolution after step 1 by Monte Carlo (MC);
3. photon pairing into π^0's by minimizing a χ^2 variable built for all possible combinations of four (i, j, k, l) out of the five photons in the event: $\chi^2 = (M_{\gamma_i\gamma_j} - M_{\pi^0})^2/\sigma^2_{M_{ij}} + (M_{\gamma_k\gamma_l} - M_{\pi^0})^2/\sigma^2_{M_{kl}}$. The mass resolution is parametrized as a function of the photon energy resolution obtained in step 2.

A second kinematic fit (KFit2) is then applied constraining also the mass of the two pions. The background rejection requires the application of two further cuts: $\chi^2_{\mathrm{KFit2}}/\mathrm{N_{dof}} < 5$ and $|\Delta M_{\pi^0}|/\sigma_{M_{\pi^0}} < 5$ for the two reconstructed π^0's. The last quantity is constructed with the output of the first kinematic fit. The signal over background ratio (S/B) evaluated at different steps of the analysis is reported in Tab. 1. The most relevant background contribution comes from $\phi \to \eta\gamma \to \pi^0\pi^0\pi^0\gamma$ events.

Data-MC comparison has been extensively studied in [2] at all analysis steps. A good agreement is found for all considered variables.

Several sources of systematics have been considered:

- **Background evaluation**
  The background contribution has been evaluated using the latest estimates on literature and KLOE measurements when available. Background-enriched distributions are used to further calibrate our expectations and check the Monte Carlo shapes. The calibration is done by fitting the data ($\mathrm{H_{data}}$) with two MC components: the

background we are considering ($\mathrm{H_{bckg}}$) and all the other contributions, including the $\pi^0\pi^0\gamma$ signal ($\mathrm{H_{others}}$): $\mathrm{H_{data}} = \alpha_1\,\mathrm{H_{bckg}} + \alpha_2\,\mathrm{H_{others}}$. A scale factor α_1 is then obtained for each background component.

- **Preselection**

  The correction to the analysis efficiency due to cosmic ray veto, background rejection and event classification (ECL) has been evaluated using prescaled data samples. A correction of 1.022 ± 0.004, mainly due to a wrong time resolution parametrization in the ECL code, is found.

- **Cluster counting**

  Two different systematics related to the cluster counting have been considered. The analysis has been repeated applying an energy scale correction of 1.4% and a new cluster efficiency curve. Contributions from angular acceptance are found to be negligible.

- **Analysis cuts**

  The analysis has been repeated by moving the χ^2_{KFit2} cut to: $\chi^2_{\mathrm{KFit2}}/\mathrm{N_{dof}} < 3$.

- **Photon pairing**

  The percentage of wrong photon pairing has been measured by fitting the difference of the two lowest value of the χ^2 used to pair photons into π^0's ($\Delta\chi^2_{\mathrm{sel}}$). The $\Delta\chi^2_{\mathrm{sel}}$ shape obtained in data has been fit using the two MC distributions obtained for events where the photons are correctly and incorrectly assigned. A factor $\varepsilon_{\mathrm{pair}}(\mathrm{data})/\varepsilon_{\mathrm{pair}}(\mathrm{MC}) = (1.08 \pm 0.02)$ is found.

The two processes $S\gamma$ and $\omega\pi$, giving the same $\pi^0\pi^0\gamma$ final state, have a very different behaviour as a function of $\sqrt{s}$: the first one is resonant, while the second one is linear, showing a dip at $\sqrt{s} \sim M_\phi$ due to the interference with ϕ decays [4]. Assuming that they are uncorrelated, it is possible to distinguish them by cutting on the ω mass: events satisfying the cut $\Delta M_\omega = |M_{\pi\gamma} - M_\omega| < 3\,\sigma_\omega$ are classified as $\omega\pi$ while all the rest is $S\gamma$. $M_{\pi\gamma}$ is the $\pi^0\gamma$ invariant mass whose value is nearer to M_ω, while $\sigma_\omega = 5$ MeV. Since these two processes cannot be completely separated, at the end of the analysis each of them is a background source for the other one. For this reason, as in [5], an iterative procedure is applied to evaluate the relative fraction of these decays, until converging to stable values. The visible cross section for the $\omega\pi$ process ($\sigma_{\pi\pi\gamma}$) has been fit with

$\sqrt{s}$ (MeV)	Run range	Luminosity (pb^{-1})
1000.10	42206–43000	106.1
1009.90	42126–42193	10.8
1018.15	42063–42113	10.2
1023.00	41908–41971	10.3
1029.95	41990–42049	11.7

Table 2: Run range and integrated luminosity for scan and off-peak data from 2005/2006 data taking.

a model independent linear parametrization and with the parametrization given by the Vector Meson Dominance Model (VMD), with a different sets of parameters for the ρ and ρ' intermediate mesons. All fit results give a huge uncertainty on the parameter describing the slope of the cross section as a function of $\sqrt{s}$. The conclusion was that a longer lever arm in the center of mass energy was needed to reliably determine it.

3 Analysis of 2005/2006 data

The analysis summarized in Par. 2 has been repeated for the scan data taken at the end of 2005 and for a fraction of the 2006 off-peak data. The list of the runs used and the corresponding center of mass energy and luminosity are reported in Tab. 2. In order to decrease the statistical error of each point, data with close $\sqrt{s}$ values are grouped together. The corresponding center of mass energy is evaluated as the weighted mean, using the luminosity as weighting factor. For the Monte Carlo sample we use the DSTs of the official 2005/2006 KLOE *omegapi* production, corresponding to an integrated luminosity five times larger than data. The most relevant differences between this MC and the RAD04 production, used for the analysis of 2001/2002 data, are the new cluster efficiency correction [6] and the usage of the correct parametrization of the time resolution in ECL (cfr. [2], Par. 7.1). For $\sqrt{s}$ values far from the ϕ peak (1000.10, 1009.90 and 1029.95 MeV) the ISR tail has been reweighted in order to reproduce the shape obtained with a standalone ISR generator for the same center of mass energy. The procedure is the same described in Ref. [2]. For each group of data listed in Tab. 2, only MC events simulated with the same center of mass energy are considered. This is important in order to reproduce

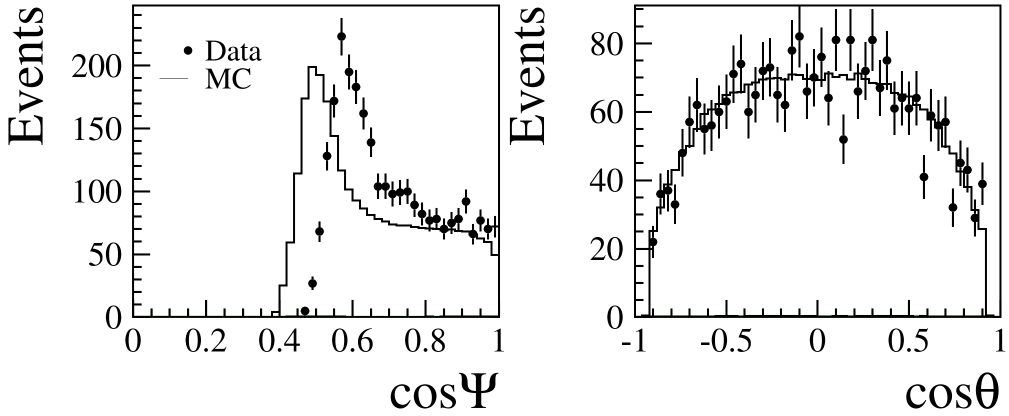

Figure 1: Angular distributions of the bachelor photon after all analysis cuts. Data are collected at $\sqrt{s} = 1000.10$ MeV while MC distributions have been generated at the ϕ mass. A data-MC difference in the shape of the $\cos\psi$ variable is clearly visible.

the angular distributions of data and to correctly evaluate the analysis efficiency. In Fig. 1 a comparison for angular distribution of the bachelor photon is done using data taken at $\sqrt{s} = 1000.10$ MeV and MC produced with a center of mass energy $\sim M_\phi$. The difference in the shape of the $\cos\psi$ variable is clearly visible.

The shape of M_ω changes as a function of $\sqrt{s}$ (see Fig. 2), thus resulting in a slope in $\varepsilon_{\rm ana}$ around the ϕ mass. The looser is the cut on the ω mass, the flatter is the efficiency. For this reason this cut has been enlarged with respect to the old analysis. The new requirement ($M_{\pi\gamma}$ cut) is that events with $750 < M_{\pi\gamma} < 830$ MeV are retained for the counting of signal. In Fig. 3.top the analysis efficiency excluding the $M_{\pi\gamma}$ cut as a function of the center of mass energy is shown for both 2001/2002 and 2005/2006 data. Since in the 2001/2002 MC production the ECL efficiency was not correctly evaluated because of a wrong parametrization in the time resolution (cfr. [2]), the ECL flag is not taken into account. A good agreement exists between the two MC samples, with a flat behaviour throughout all the $\sqrt{s}$ spanned region. A residual $\sqrt{s}$ dependence is instead clearly visible on the $M_{\pi\gamma}$ cut (Fig. 3.bottom).

The good data-MC comparison obtained for 2001/2002 data is confirmed with scan

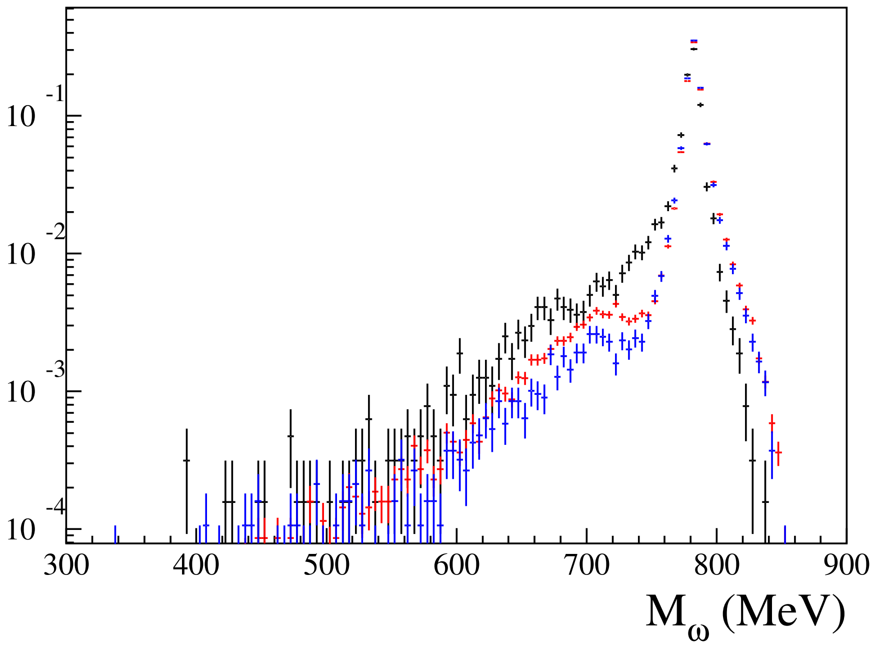

Figure 2: Simulated ω mass shape for different center of mass energies: 1000.10 MeV (black), 1019.30 MeV (red) and 1019.90 MeV (blue).

and off-peak data (see Figs. 4-8). Data taken at 1000.10, 1009.90 and 1029.95 MeV are essentially background free. The agreement for these $\sqrt{s}$ values shows that the signal parametrization and its behaviour as a function of the center of mass energy is correctly described by our simulation. As a further check, a data-MC comparison for all energy and angular distributions is reported in Figs. 9, 10 for data taken at 1000.10 MeV data.

4 Preselection efficiency for 2005/2006 data

As in 2001/2002 data analysis, efficiency corrections due to cosmic ray veto, FILFO and event classification have been evaluated using prescaled data samples.

Since in 2002 a T3 filter recovering cosmic veto losses was implemented, the cosmic ray veto efficiency changed between 2001 and 2002 data. In order to be fully consistent for the analysis of the two data sets, events with a CV flag in data were not considered

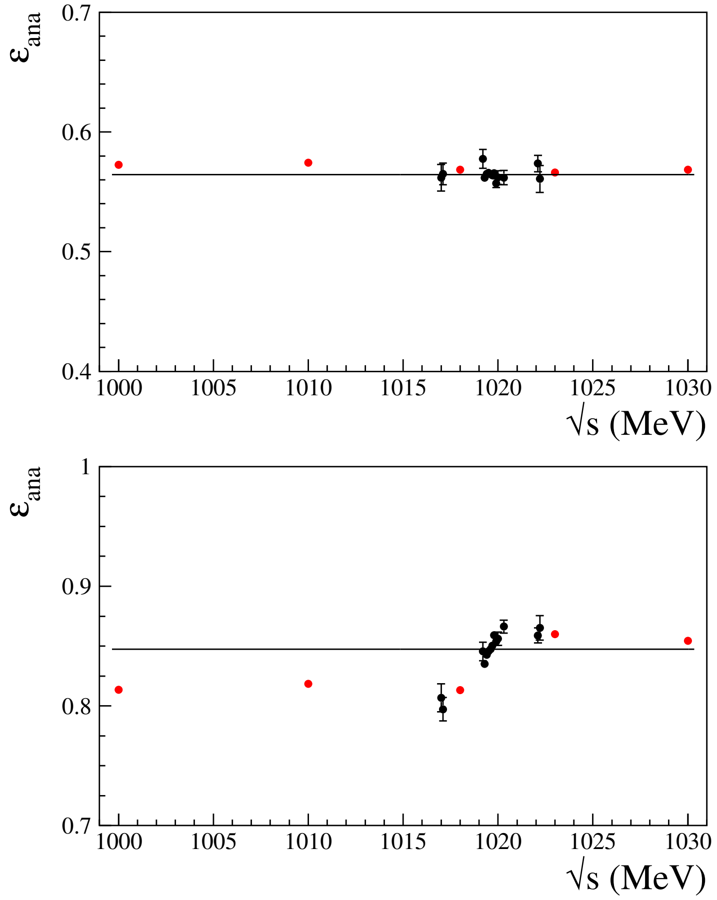

Figure 3: Analysis efficiency as a function of the center of mass energy, evaluated using KLOE official MC production. Top: after sample selection and χ^2_{Kfit2}, ΔM_{π^0} cuts. Bottom: efficiency due to the application of the $M_{\pi\gamma}$ cut only. Black (red) points are 2001/2002 (2005/2006) data.

in the analysis of 2002 data and a common correction obtained from the 2001 prescaled events [1] was applied. The same procedure is applied for 2005/2006 data. In order to check the consistency with the old data set, the fraction of events with a CV flag is measured both for 2002 and 2005/2006 events. The two numbers are fully consistent:

[1] In the streamed data the events rejected by the cosmic veto are retained with a prescaling factor of 50.

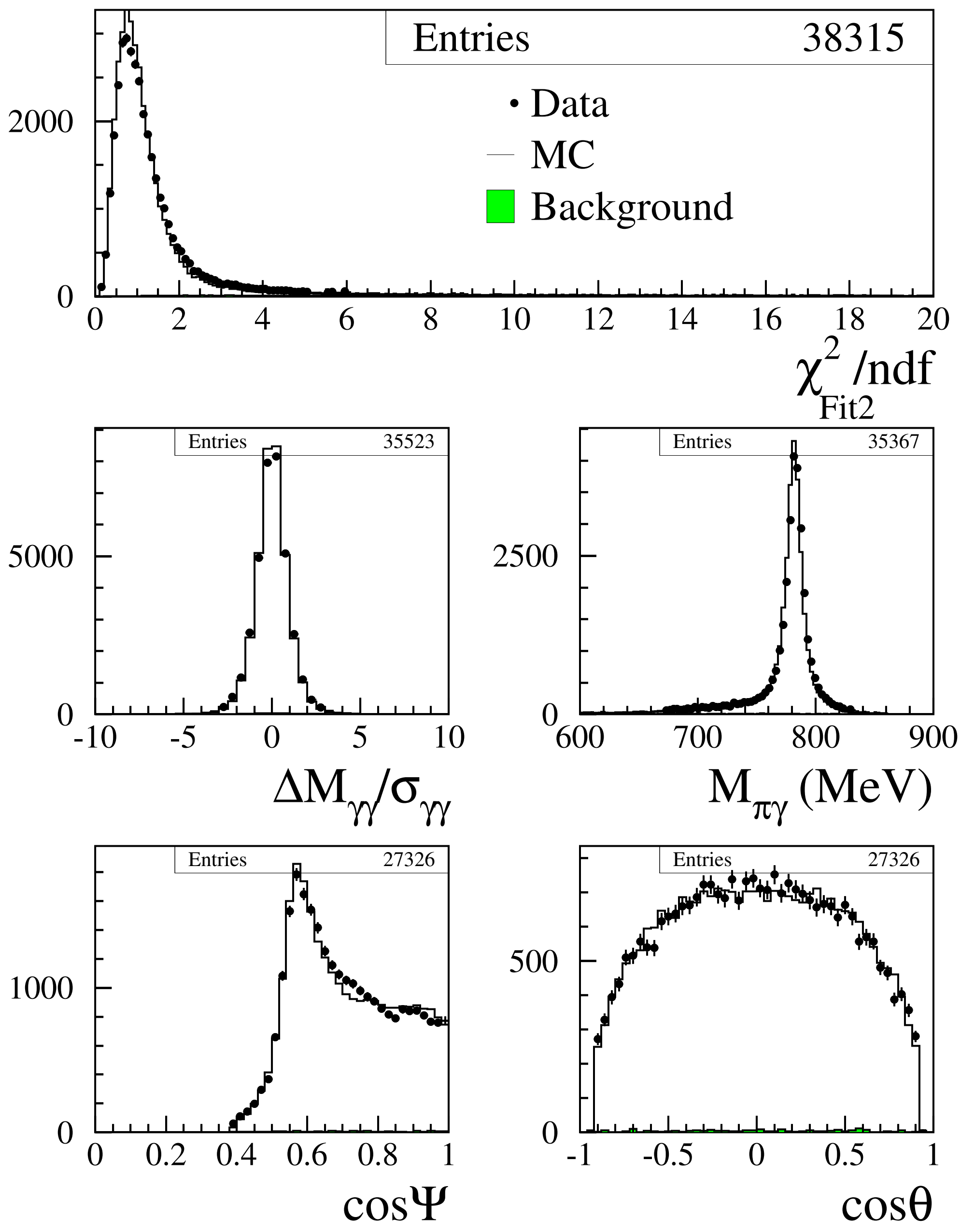

Figure 4: Data-MC comparison using data taken at $\sqrt{s} = 1000.10$ MeV. Top: χ^2 of the second kinematic fit after sample selection. Center-left: normalized two photon invariant mass after $\chi^2_{\rm Fit2}$ cut. Center-right: $\pi^0\gamma$ invariant mass after $\Delta M_{\gamma\gamma}$ cut. Bottom: angular distributions of the bachelor photon after all analysis cuts.

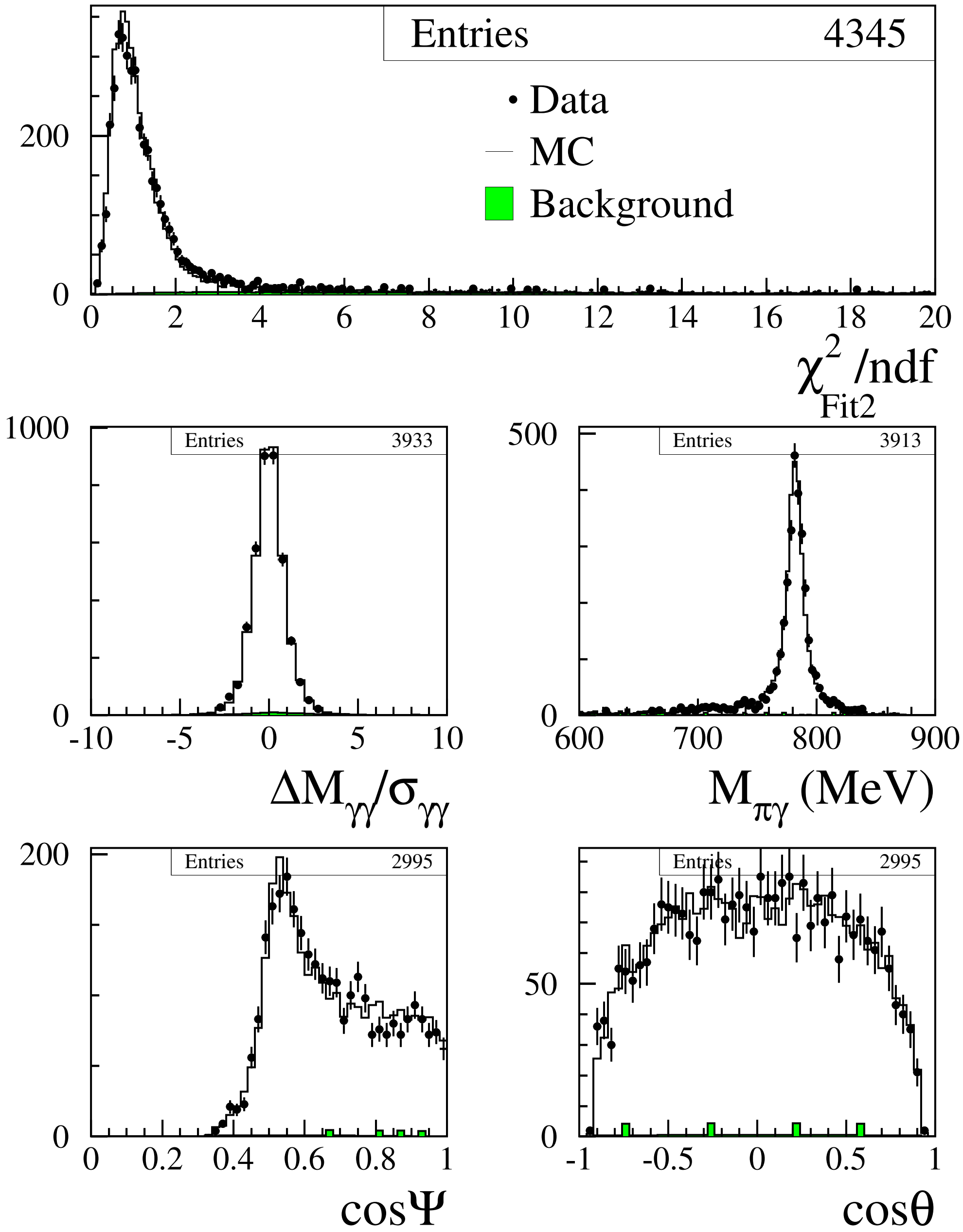

Figure 5: Data-MC comparison using data taken at $\sqrt{s} = 1009.90$ MeV. Top: χ^2 of the second kinematic fit after sample selection. Center-left: normalized two photon invariant mass after $\chi^2_{\rm Fit2}$ cut. Center-right: $\pi^0\gamma$ invariant mass after $\Delta M_{\gamma\gamma}$ cut. Bottom: angular distributions of the bachelor photon after all analysis cuts.

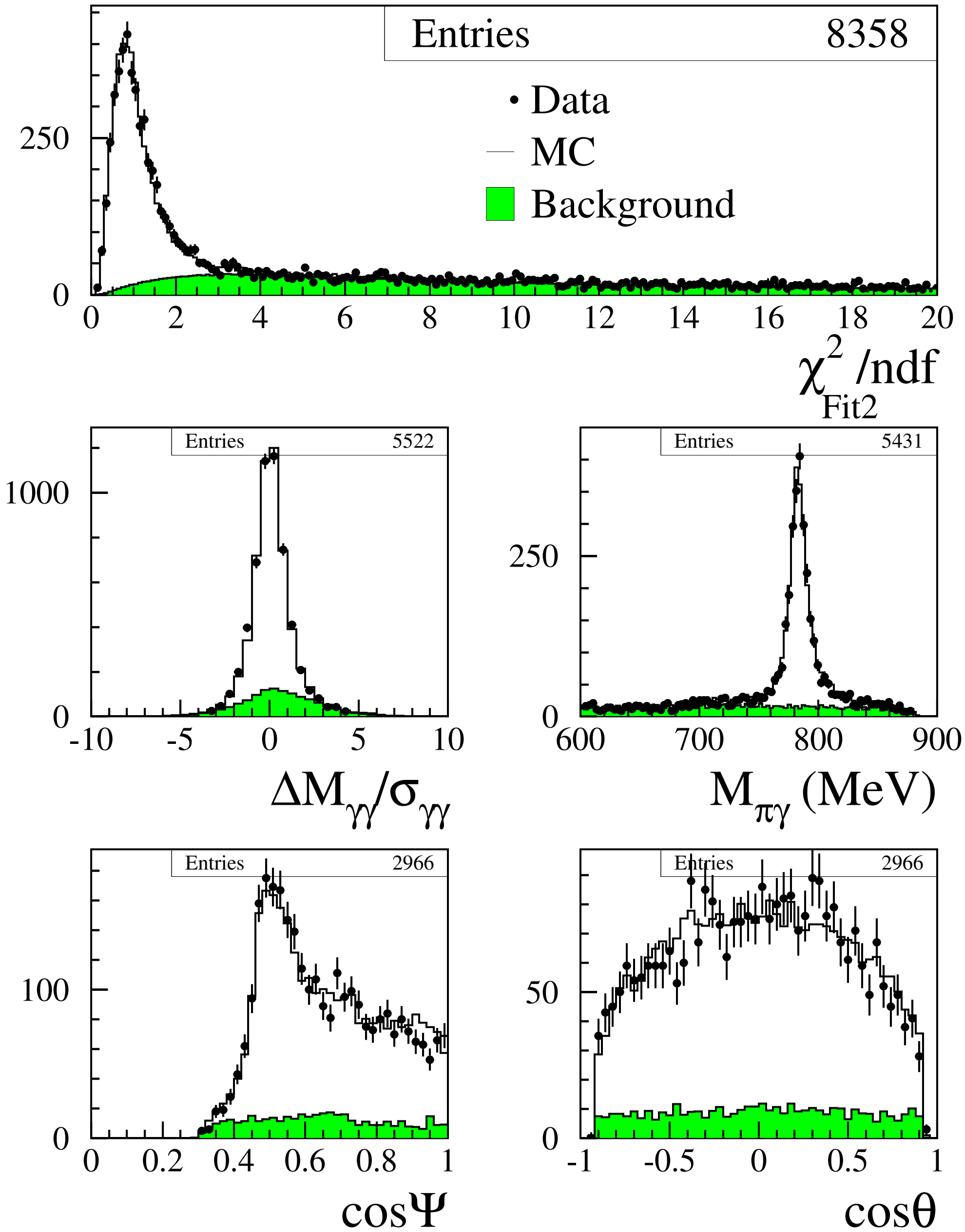

Figure 6: Data-MC comparison using data taken at $\sqrt{s} = 1018.15$ MeV. Top: χ^2 of the second kinematic fit after sample selection. Center-left: normalized two photon invariant mass after $\chi^2_{\rm Fit2}$ cut. Center-right: $\pi^0\gamma$ invariant mass after $\Delta M_{\gamma\gamma}$ cut. Bottom: angular distributions of the bachelor photon after all analysis cuts.

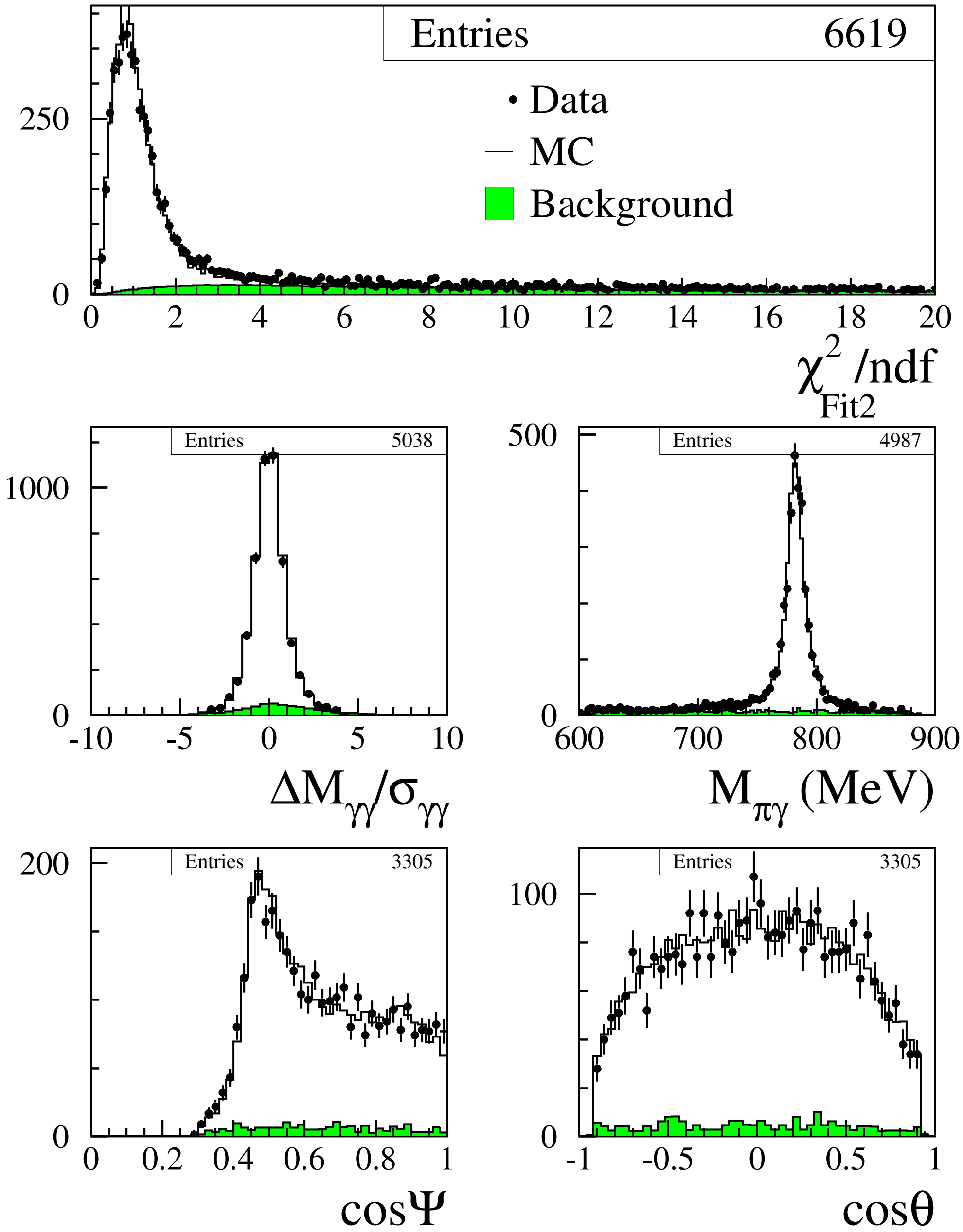

Figure 7: Data-MC comparison using data taken at $\sqrt{s} = 1023.00$ MeV. Top: χ^2 of the second kinematic fit after sample selection. Center-left: normalized two photon invariant mass after χ^2_{Fit2} cut. Center-right: $\pi^0\gamma$ invariant mass after $\Delta M_{\gamma\gamma}$ cut. Bottom: angular distributions of the bachelor photon after all analysis cuts.

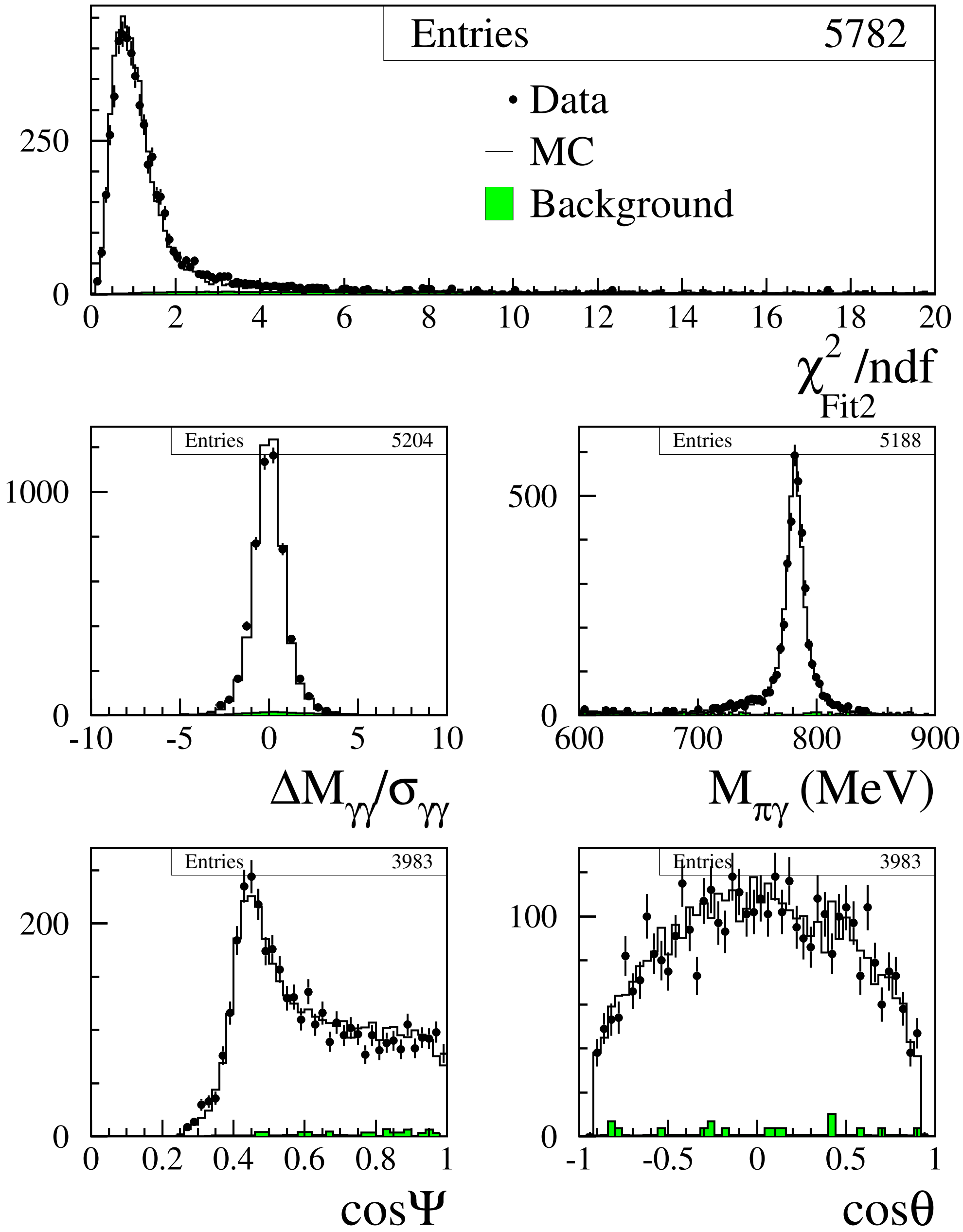

Figure 8: Data-MC comparison using data taken at $\sqrt{s} = 1029.95$ MeV. Top: χ^2 of the second kinematic fit after sample selection. Center-left: normalized two photon invariant mass after χ^2_{Fit2} cut. Center-right: $\pi^0\gamma$ invariant mass after $\Delta M_{\gamma\gamma}$ cut. Bottom: angular distributions of the bachelor photon after all analysis cuts.

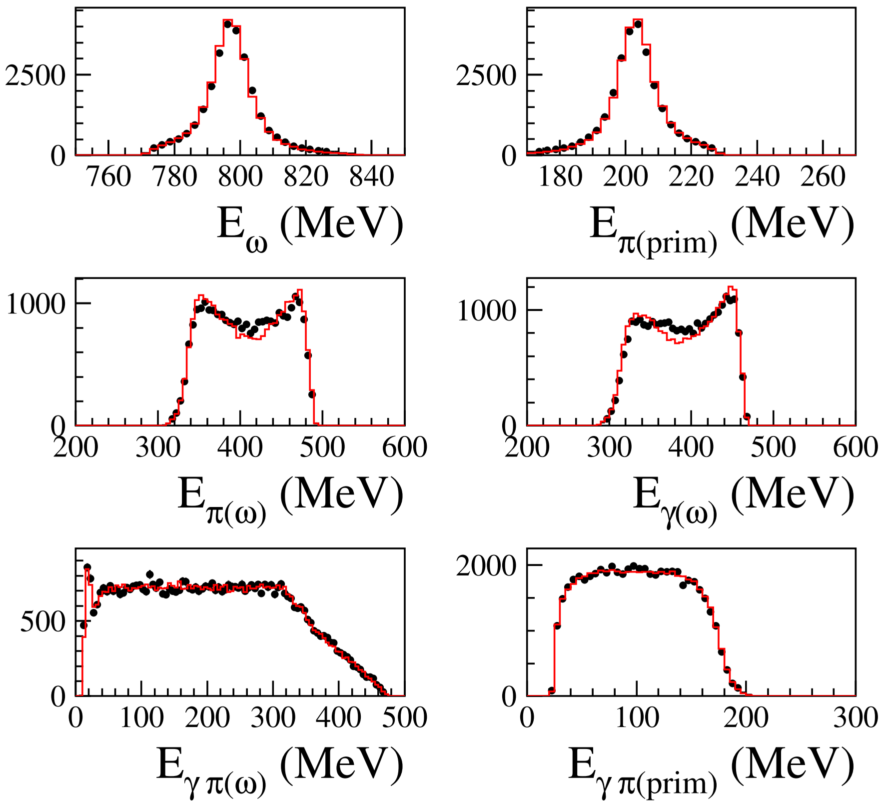

Figure 9: Data-MC comparison of energy distributions for $e^+e^- \to \omega\pi^0 \to \pi^0\pi^0\gamma$ events taken at $\sqrt{s} = 1000.10$ MeV after background subtraction. Top: energy spectrum for ω and π^0 produced in the collision. Center: energy spectrum for the π^0 and γ produced in the radiative decay of the ω. Bottom: distribution of the photon energy spectrum for the γ's coming from the π^0 from ω and for the primary π^0.

$\varepsilon_{\rm CV}(2005/2006) = (99.965 \pm 0.007)\%\,,\ \varepsilon_{\rm CV}(2002) = (99.956 \pm 0.008)\%\,.$

The Event Classification (ECL) efficiency has been evaluated directly from data using the new UFO stream, where events passing the machine background filter (FILFO) are retained with a scale factor 1:20. For the off-peak data, only 30 pb^{-1} have been used, corresponding to runs 42501–42700. In Tab. 3, the number of events surviving the anal-

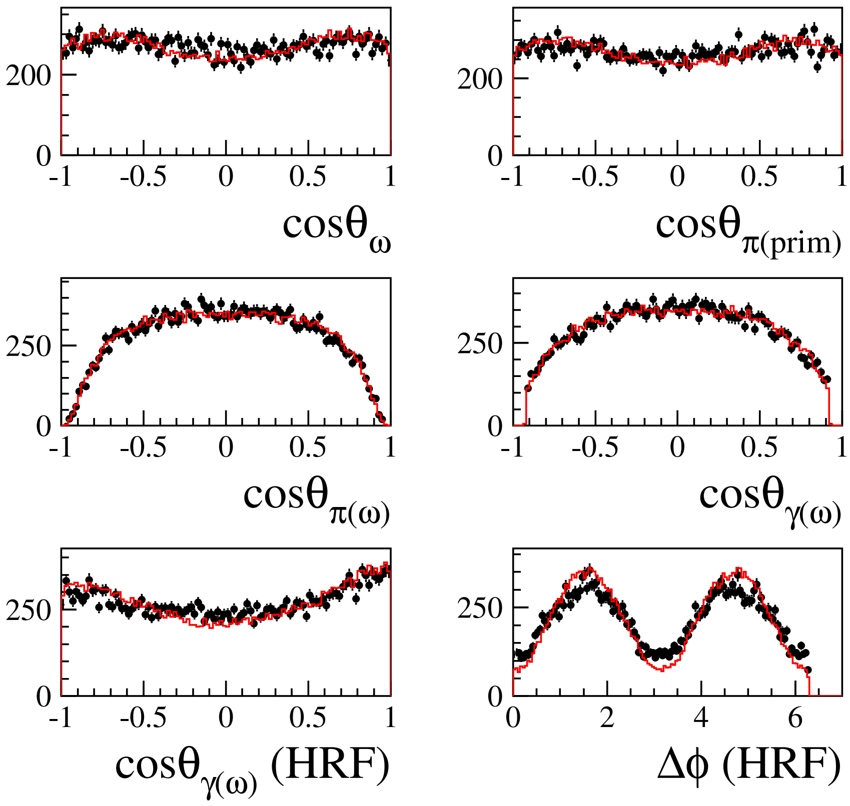

Figure 10: Data-MC comparison of angular distributions for $e^+e^- \to \omega\pi^0 \to \pi^0\pi^0\gamma$ events taken at $\sqrt{s} = 1000.10$ MeV after background subtraction. Top: polar angle for ω and π^0 produced in the collision. Center: polar for the π^0 and γ produced in the radiative decay of the ω. Bottom: distribution of $\cos\theta_{\gamma(\omega)}$ and $\Delta\phi$ evaluated in the helicity rest frame.

ysis cuts ($\mathrm{N_{tot}}$) and also the ECL algorithm ($\mathrm{N_{ECL}}$) are reported together with the ECL efficiency. Since the correction is small and the efficiencies obtained for different $\sqrt{s}$ are in agreement, we use the value $\varepsilon_{\mathrm{ECL}} = (99.5 \pm 0.3)\%$, obtained by grouping together all center of mass energies. As a cross check, we evaluate the ECL efficiency also for MC events. The values, reported in Tab. 3, are in agreement with the output of UFO stream.

The FILFO efficiency has been measured by Monte Carlo, both for different $\sqrt{s}$ values

DATA			
$\sqrt{s}$ (MeV)	N_{tot}	N_{ECL}	ε_{ECL}
All	792	788	$(99.5 \pm 0.3)\%$
1000.10	251	249	$(99.2 \pm 0.6)\%$
1009.90	126	126	$(\pm)\%$
1018.15	113	112	$(99.1 \pm 0.9)\%$
1023.00	124	123	$(99.2 \pm 0.8)\%$
1029.95	178	178	$(\pm)\%$
MONTE CARLO			
$\sqrt{s}$ (MeV)	N_{tot}	N_{ECL}	ε_{ECL}
All	156170	154940	$(99.21 \pm 0.02)\%$
1000.10	102820	101970	$(99.17 \pm 0.03)\%$
1009.90	13827	13712	$(99.17 \pm 0.08)\%$
1018.15	12063	11985	$(99.35 \pm 0.07)\%$
1023.00	12786	12707	$(99.38 \pm 0.07)\%$
1029.95	14725	14613	$(99.24 \pm 0.07)\%$

Table 3: Event Classification efficiency for 2005/2006 data evaluated using the UFO stream and MC events.

and by grouping together all 2005 MC events. The resulting values are fully consistent. The mean value $\varepsilon_{\rm FLF} = (99.917 \pm 0.007)\%$ is in good agreement with the number obtained for 2001/2002 data, using both MC and a minimum bias samples.

5 Fit to the $\sqrt{s}$ dependence of the visible cross section

There are some differences in the analysis an in the evaluation of the $e^+e^- \to \omega\pi^0 \to \pi^0\pi^0\gamma$ visible cross section comparing with the procedures used for the 2001/2002 data only:

1. the evaluation of the integrated luminosity for each $\sqrt{s}$ point has been done taking into account the dependence of the Bhabha cross section as a function of the center of mass energy;

2. the new curves of the cluster efficiency correction have been applied also to the

2001/2002 MC production;

3. as discussed in Par. 3, the three σ's cut around the ω mass has been changed to $750 < M_{\pi\gamma} < 830$ MeV;

4. the efficiency and the signal/background shapes have been obtained by MC using events simulated with the same center of mass energy;

5. except for luminosity and preselection, systematic errors are not added to the statistical ones of the visible cross section as in the past.

For each $\sqrt{s}$ value, the integrated luminosity, the number of events after all the analysis cuts, the expected background and the visible cross section are reported in Tab. 4. The dependence of the cross section on the center of mass energy has been parametrized in the form [4]:

$$\sigma(\sqrt{s}) = \sigma_{NR}(\sqrt{s}) \cdot \left| 1 - Z \frac{M_\phi \Gamma_\phi}{D_\phi} \right|^2 \tag{1}$$

where $\sigma_{NR}(\sqrt{s})$ is the bare cross section for the non-resonant process, Z is the complex interference parameter (i.e. the ratio between the ϕ decay amplitude and the other processes), while M_ϕ, Γ_ϕ and D_ϕ are the mass, the width and the inverse propagator of the ϕ meson respectively. Since in the considered center of mass energy range the non-resonant cross section increases almost linearly, the visible cross section for the $\omega\pi$ process has been fit with the model independent linear parametrization:

$$\sigma_{NR}(\sqrt{s}) = \sigma_0 + \sigma'(\sqrt{s} - M_\phi) \tag{2}$$

Fit results are reported in the first line of Tab. 5. The corresponding normalized correlation coefficients are:

	σ_0	$\Re(Z)$	$\Im(Z)$	σ'
σ_0	1.000	−0.303	−0.855	0.874
$\Re(Z)$		1.000	0.137	−0.444
$\Im(Z)$			1.000	−0.633
σ'				1.000

We have repeated the fit using for the bare cross section the VMD description based on ρ and ρ' intermediate states [4]. Results are in agreement with the linear parametrization within one standard deviation.

$\sqrt{s}$ (MeV)	$L_{\rm int}$ (pb^{-1})	N	B	$\sigma_{\pi\pi\gamma}$ (nb)
1000.10	106.1	27326 ± 165	216 ± 20	0.550 ± 0.005
1009.90	10.8	2995 ± 55	37 ± 8	0.581 ± 0.012
1017.20	7.4	2108 ± 46	204 ± 9	0.564 ± 0.018
1018.15	10.2	2966 ± 54	409 ± 16	0.541 ± 0.014
1019.30	1.4	397 ± 20	75 ± 4	0.480 ± 0.034
1019.45	26.5	7488 ± 87	1430 ± 35	0.497 ± 0.009
1019.55	41.9	11776 ± 109	2260 ± 53	0.487 ± 0.008
1019.65	76.9	22507 ± 150	4158 ± 95	0.509 ± 0.007
1019.75	143.7	41836 ± 205	7787 ± 174	0.505 ± 0.006
1019.85	109.5	31977 ± 179	5854 ± 131	0.508 ± 0.006
1019.95	15.1	4311 ± 66	801 ± 21	0.491 ± 0.011
1020.05	7.6	2227 ± 47	384 ± 11	0.516 ± 0.016
1020.15	3.0	846 ± 29	144 ± 5	0.501 ± 0.024
1020.45	2.9	806 ± 28	139 ± 6	0.488 ± 0.024
1022.30	5.9	1891 ± 43	157 ± 7	0.612 ± 0.018
1023.00	10.3	3305 ± 57	204 ± 14	0.619 ± 0.013
1029.95	11.7	3983 ± 63	87 ± 14	0.689 ± 0.013

Table 4: Summary table for $\omega\pi$ events as a function of $\sqrt{s}$: integrated luminosity ($L_{\rm int}$), number of events (N), expected background (B). In the last quantity, the errors include both the MC statistics and the uncertainty on background BRs. In the last column, the $e^+e^- \to \omega\pi^0 \to \pi^0\pi^0\gamma$ visible cross section is reported. The error on $\sigma_{\pi\pi\gamma}$ include MC statistics, background BRs and luminosity and preselection uncertainties.

6 Systematics on fit results

The systematics effects that have been taken into account are the following:

1. **$\chi^2_{\rm Fit2}$ cut**
   The analysis has been repeated by moving the $\chi^2_{\rm KFit2}$ cut to: $\chi^2_{\rm KFit2}/{\rm N_{dof}} < 3\,.$

2. **$M_{\pi\gamma}$ cut**
   The analysis has been repeated by moving the cut on the ω mass to:

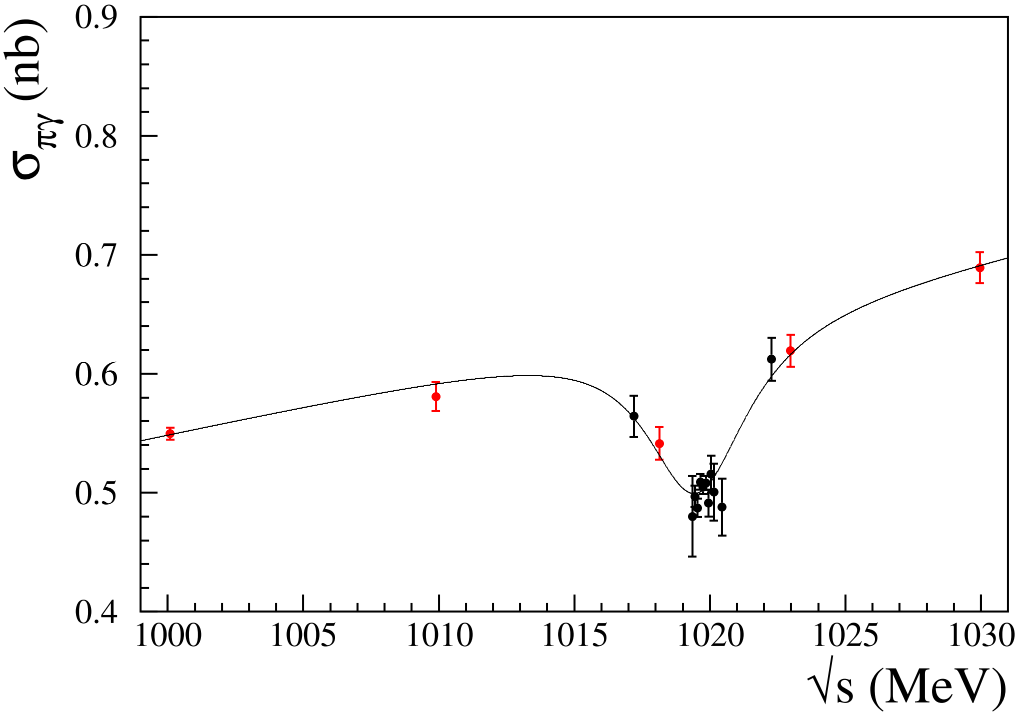

Figure 11: Fit to the $e^+e^- \to \omega\pi^0 \to \pi^0\pi^0\gamma$ visible cross section. Black (red) points are 2001/2002 (2005/2006) data.

$$\Delta M_\omega = |M_{\pi\gamma} - M_\omega| < 3\,\sigma_\omega\,.$$

3. ***E_γ* cut**

   The analysis has been repeated using a higher threshold on the cluster energy in the photon counting: $E_\gamma > 20$ MeV.

4. **Energy scale**

   The analysis has been repeated applying the energy scale correction of 1.4% to MC events.

5. **Background**

   The analysis has been repeated applying the scale factors to the background.

6. **$\sqrt{s}$ scale**
   The fit has been repeated shifting the $\sqrt{s}$ value of -150 keV.

7. **ISR tail**
   The fit has been repeated by using the same ISR tail for all $\sqrt{s}$ values

8. **$M_{\pi\pi}$ shape**
   The reshaping of the $M_{\pi\pi}$ distribution for $e^+e^- \to \omega\pi^0 \to \pi^0\pi^0\gamma$ events, which takes into account a typo in the VMD description, has been removed.

9. **Interference with $\phi \to S\gamma$**
   From the fit to the $\pi^0\pi^0\gamma$ Dalitz plot an interference term between the $\phi \to S\gamma$ and the $e^+e^- \to \omega\pi^0 \to \pi^0\pi^0\gamma$ process has been extracted. Its contribution, evaluated for each $\sqrt{s}$ value, has been subtracted to the visible cross section.

For each systematics, new values of the visible cross section are obtained after having applied the corresponding cut/correction and its dependence on $\sqrt{s}$ is fitted. Results are reported in Tab. 5. The systematic error is defined as the RMS of the extracted parameters. The final result is therefore:

$$\sigma_0 = (\,0.724 \pm 0.010 \pm 0.003\,)\ \text{nb} \tag{3}$$
$$\Re(Z) = 0.011 \pm 0.015 \pm 0.006 \tag{4}$$
$$\Im(Z) = -0.154 \pm 0.007 \pm 0.004 \tag{5}$$
$$\sigma' = (\,0.0053 \pm 0.0005 \pm 0.0002\,)\ \text{nb/MeV} \tag{6}$$

7 Conclusions

From a fit to the center of mass energy dependence of $e^+e^- \to \omega\pi^0 \to \pi^0\pi^0\gamma$ events, the parameters describing the effective cross section are extracted. This work, together with the analogous study on the $e^+e^- \to \omega\pi^0 \to \pi^+\pi^-\pi^0\pi^0$ channel, allows to measure the ratio of the width for the two main ω decays: $\Gamma(\omega \to \pi^0\gamma)/\Gamma(\omega \to \pi^+\pi^-\pi^0)$. Since these final states correspond to $\sim 98\%$ of the ω decay channels, this ratio and the sum of the residual rarer BR measurements [7] are used to extract the main ω branching fractions

Fit type	σ_0 (nb)	$\Re(Z)$	$\Im(Z)$	σ' (nb/MeV)	χ^2/Ndf
Standard	0.724 ± 0.010	0.011 ± 0.015	-0.154 ± 0.007	0.0053 ± 0.0005	11.79/13
$\chi^2_{\rm Fit2}$ cut	0.720 ± 0.011	0.004 ± 0.017	-0.155 ± 0.007	0.0054 ± 0.0006	8.72/13
M_ω cut	0.730 ± 0.010	0.005 ± 0.015	-0.156 ± 0.007	0.0059 ± 0.0005	7.30/13
E_γ cut	0.727 ± 0.012	0.010 ± 0.015	-0.155 ± 0.008	0.0055 ± 0.0006	8.77/13
En. scale	0.722 ± 0.011	0.004 ± 0.015	-0.155 ± 0.007	0.0054 ± 0.0005	8.95/13
Bckg.	0.724 ± 0.012	0.012 ± 0.015	-0.157 ± 0.008	0.0053 ± 0.0006	12.56/13
$\sqrt{s}$ scale	0.723 ± 0.011	0.022 ± 0.015	-0.151 ± 0.007	0.0052 ± 0.0005	11.28/13
ISR tail	0.728 ± 0.011	0.010 ± 0.015	-0.158 ± 0.007	0.0052 ± 0.0005	11.17/13
$M_{\pi\pi}$ shape	0.728 ± 0.011	0.006 ± 0.015	-0.153 ± 0.007	0.0054 ± 0.0005	10.06/13
Interf.	0.724 ± 0.012	0.019 ± 0.015	-0.168 ± 0.008	0.0052 ± 0.0006	11.72/13

Table 5: Fit results for $e^+e^- \to \omega\pi^0 \to \pi^0\pi^0\gamma$ cross section. The first line is the output of the standard analysis while the other ones are the results of systematic studies.

imposing the unitarity. Results are reported in [3], and are used to evaluate the branching fraction for the OZI and G-parity violating decay $\phi \to \omega\pi^0$.

References

[1] F. Ambrosino *et al.*, KLOE Collaboration, Eur. Phys. J. C 49 (2007) 473.

[2] S. Giovannella and S. Miscetti, "Study of the $e^+e^- \to \pi^0\pi^0\gamma$ process using 2001/2002 data", KLOE Note 212 (2006).

[3] A. De Santis and S. Giovannella, "Study of $e^+e^- \to \omega\pi^0 \to \pi^+\pi^-\pi^0\pi^0$ process using KLOE data", KLOE Memo 344 (2008).

[4] V. M. Aulchenko *et al.*, J. Exp. Th. Phys. 90 (2000) 927-938.

[5] S. Giovannella and S. Miscetti, KLOE Note 178 (2002).

[6] C. Gatti, M. Palutan and T. Spadaro, KLOE Note 209 (2006).

[7] W. M. Yao *et al.*, J. Phys. G 33 (2006) and 2007 partial update for 2008 edition [*http://pdg.web.cern.ch/pdg*]